Interferometric Measurement of Neutron Fizeau Effect

Ulrich Bonse and Andreas Rumpf[a]

Institute for Physics, University of Dortmund, 4600 Dortmund 50, Federal Republic of Germany

(Received 18 November 1985)

For thermal neutrons we have measured the Fizeau effect to 1.5% accuracy. The quoted accuracy was achieved by use of a newly designed neutron interferometer. Four fast-moving samples, all parts of a single, four-winged, aluminum, rotating propeller, could be made to engage simultaneously in the interfering beams. Our experiment complements and exceeds two recent Fizeau experiments, one of which was performed with cold neutrons and much lower accuracy and the other with a moving medium inside stationary boundaries resulting in a null Fizeau effect.

PACS numbers: 03.30.+p, 61.12.Gz

The "dragging effect" of light in moving media was first observed by Fizeau in 1851.[1,2] The outcome of the measurement was considered a triumph of Fresnel's idea of partial ether dragging by matter. Later the Fizeau effect was shown to follow from special relativity,[3,4] and a number of more elaborate experiments with light were performed.[5–7] However, as Lerche[8] has pointed out, the accuracy obtained in those investigations is insufficient to distinguish experimentally between the competing formulas of Fresnel and Lorentz for the Fizeau effect of light.

On the other hand, the neutron Fizeau effect is not likely to bear directly on special relativity. The reason being that thermal (or cold) neutrons move at speeds small compared to the velocity of light c. However, neutron Fizeau experiments are capable of illustrating and verifying the physics of the transformation laws in wave mechanics.[9–11]

In a beautiful experiment Arif *et al.*[12] confirmed the null result for the case when the medium is moving inside stationary boundaries, by rotating a quartz disk in a thermal-neutron interferometer.

Klein *et al.*[13] measured the neutron Fizeau effect in a double-slit diffraction experiment using cold neutrons. The accuracy of that experiment was limited to about 10%. Therefore, a more accurate comparison with the theory of the neutron Fizeau effect has been desirable. Furthermore, we felt it important to measure the effect at thermal neutron energies.

A very precise way to measure thermal-neutron phase shifts is to employ perfect-crystal interferometers.[14–16] In our case the S18 neutron interferometer installed at the high-flux reactor of the Institut Laue-Langevin in Grenoble was used. With standard interferometer crystals beam splitting and beam recombination is achieved by Bragg diffraction in the Laue geometry. Relative phase shifts occurring along the paths of the two interfering beams inside the interferometer cause intensity (counting rate) variations which may generally be fitted by a function

$$Y = A + B\cos(CX + P). \tag{1}$$

Here Y is the counting rate, X is the neutron-optical path difference of the interfering beams, and A, B, C, and P are fit parameters. We call P_0 the phase determined by the fitting procedure with the sample at rest. When the sample movement is switched on, a velocity-dependent phase shift $\Delta\Phi$ is induced, so that

$$P = P_0 + \Delta\Phi. \tag{2}$$

In order to perform a precision measurement of the Fizeau effect we needed high sensitivity to velocity-induced phase shifts which means large sample speeds. At the same time, in order to preserve high contrast of the interference fringe pattern, vibration transmission from the sample movement to the interferometer itself had to be minimized. Both goals could be achieved by our employing a rotating sample rather than one which performs linear motions in an oscillating fashion, and giving the sample the shape of a four-winged propeller combined with the special interferometer design as shown in Figs. 1 and 2.

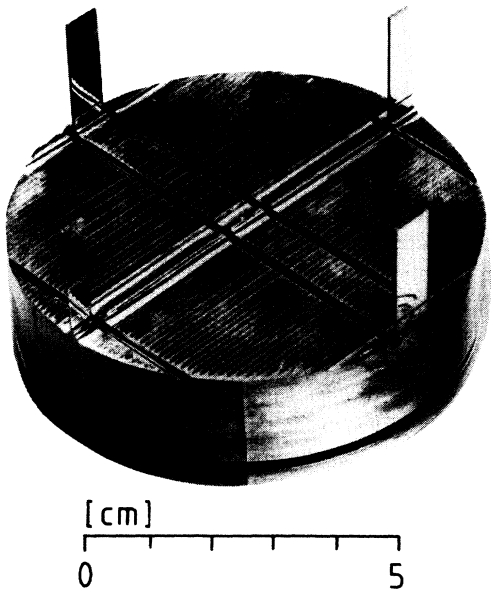

FIG. 1. Photograph of interferometer crystal.

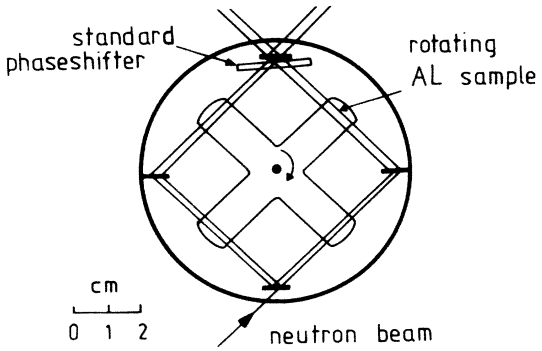

FIG. 2. Layout of beams and specimen shape with the new square-geometry interferometer. See text.

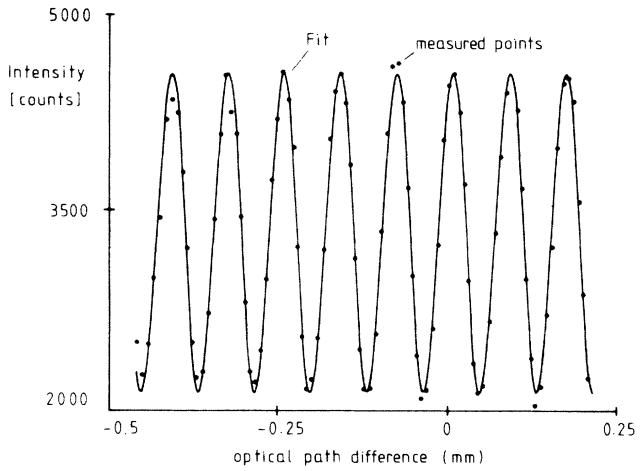

FIG. 3. Typical interference fringe pattern. Contrast equals about 37%.

The new interferometer (manufactured at the University of Dortmund) has four separate wafers each 24 mm high, 0.64 mm thick, and about 7 mm wide which act as beam splitter, mirrors, and beam-superimposing analyzer. If the Bragg angle is $\Theta_B = \pi/4$, a neutron wavelength of $\lambda = 1.92$ Å is obtained from the 400 reflection in silicon, and the interfering beams follow the geometry of a perfect square. Thus the four 10-mm-thick propeller wings engage simultaneously in the interfering beams. It is easily seen that the velocity-induced phase shifts of all wings add with equal sign so that a factor of 4 in sensitivity is obtained. The propeller itself is completely encapsulated inside an aluminum box 65 mm by 65 mm wide for which there is enough free space between the crystal wafers. The box is fitted with Mylar windows at the entrance and exit points of the neutron beams. In front of the analyzer crystal a tantalum plate is inserted which serves as a standard phase shifter. A typical interference fringe pattern measured with the new interferometer is shown in Fig. 3. Although the beam splitter, mirrors, and analyzer are quite small and fairly wide apart, the interference contrast is still about 37%.

The propeller is rotated by a stepping motor via a 1-m-long shaft in order to reduce disturbances due to the motor. The counting rates of the outgoing neutron beams are sorted into a multichannel analyzer by an angular encoder combined with a special electronic system. Only over the four angular regions where the wings engage fully in the beams is the interference pattern observed.

In our calculation,[11] assuming a parallel-sided specimen as explained in Fig. 4, we transform the time-dependent Schrödinger equation to the frame at rest with the specimen's boundary and determine the neutron wave function by applying time-independent boundary conditions in that frame. In our measurement, the velocity v_a of the scattering atoms equals the velocity v_b of the boundary. Therefore, angles ξ and η in Fig. 4 are equal. Furthermore, assuming the bound coherent nuclear scattering length b_c to be independent of the neutron wave vector, which in the thermal-neutron range holds for most materials to high accuracy, we obtain for the measurable speed-induced phase shift caused by the specimen of Fig. 4

$$\Delta\Phi = -C_b v_b, \tag{3}$$

with

$$C_b = [4\pi^2 N d b_c m \cos(\theta - \eta)]/[hK_i^2 \cos^2\theta]. \tag{4}$$

K_i is the incident neutron's wave vector, N is the number of scattering atoms per unit volume, m is the neutron rest mass, and h is Planck's constant. θ, η, and d are explained in Fig. 4.

It follows from Eq. (4) that the phase shift is zero when the velocity v_b is parallel to the specimen surface. This was recently verified experimentally by Arif *et al.*[12] in their null Fizeau-effect experiment. As was

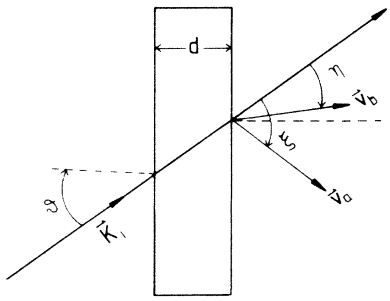

FIG. 4. Neutron beam with incident wave vector $\mathbf{K}_i$ traversing a parallel-sided specimen, the scattering atoms of which move with velocity $\mathbf{v}_a$ while the boundaries have velocity $\mathbf{v}_b$.

already pointed out by Arif *et al.*, with v_b parallel to the surface the phase shift is proportional to $\partial b_c/\partial K$ which in principle could thus be measured by a tuning of K via v_b, where K is the neutron's wave vector seen from the scattering atoms. Assuming the specimen to be a rotating disk with rotation axis parallel to the neutron beam which passes the disk at a distance $r = 10$ mm from its axis, we calculate $\nu = 3\times 10^5$ rpm to be necessary in order to obtain a tuning range of 10% at a 2-Å neutron wavelength. Such a speed does not seem feasible. Nevertheless, a tuning range of a few percent appears to be attainable by this method.

From the numbers of the corresponding channels of the multichannel analyzer we calculate the variation of θ (Fig. 4) occurring over each of the fringe-yielding regions. We then use the average of $v_b/(\cos^2\theta)$ over the range -0.307 rad $< \theta < +0.307$ rad in Eqs. (3) and (4). The total thickness of all four wings was $d = 0.0398(1)$ m.

The scattering-length density Nb_c of the propeller material was directly measured by rotating one of the wings within a pair of nonparallel interfering beams and recording the fringe pattern as a function of rotation angle. Nb_c is then determined from the period of the fringe pattern. It was found that

$$Nb_c(\text{sample}) = 2.085(4)\times 10^{14}\ \text{m}^{-2}, \tag{5}$$

whereas[17]

$$Nb_c(\text{pureAl}) = 2.077(3)\times 10^{14}\ \text{m}^{-2}. \tag{6}$$

Similarly the wavelength used was directly determined by Fourier transformation of the interference pattern[18] of a standard aluminum phase plate with a known Nb_c value. We found

$$\lambda = 1.9265(30)\ \text{Å}. \tag{7}$$

Since for aluminum at this wavelength, $\partial b_c/\partial K = 0$, we thus have all the parameters at hand to calculate the theoretical phase shift according to Eq. (3).

The motion-induced phase shift depends on the total thickness of the material present in all four beams, whereas the initial phase depends on the thickness difference of materials in the two interfering beams. When the propeller makes a turn of 360° there are four positions, at 90° intervals, where the wings engage fully into the beams. Because of manufacturing tolerances of the propeller wings the four positions yield slightly different initial phases. The measurements were therefore made in the following way.

Interference fringe patterns were recorded alternately with the propeller rotating quickly (i.e., at speeds for which the motion-induced shift was to be measured) and with the propeller rotating slowly (i.e., at a speed for which the motion-induced phase shift is practically zero). Motion-induced phase shifts were then determined for the four propeller positions separately by subtraction of the phase obtained from the quasistatic measurement from that obtained with the propeller rotating at various speeds.

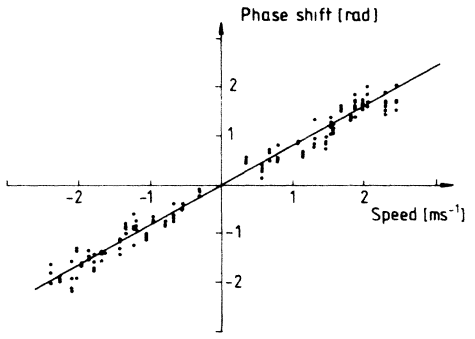

FIG. 5. Linear fit of 147 motion-induced phase-shift measurements. See text.

In this way 147 motion-induced phase shifts $\Delta\Phi(v_b)$ were measured with specimen speed differences v_b ranging from -2.4 to $+2.4$ m s^{-1}. Separate linear fits with Eq. (3) for the four different angular positions gave $C_b = 0.8016$, 0.8112, 0.7893, 0.8038 rad s m^{-1}, respectively. Since the differences among the C_b are within one standard deviation they may be fitted simultaneously (Fig. 5), giving

$$C_{b\,\text{expt}} = 0.8012(0.01)\ \text{rad s m}^{-1}. \tag{8}$$

The experimental error, which includes fit statistics and errors of λ, Nb_c, etc., amounts to about 1.5%. This is roughly 1 order of magnitude more accurate than the cold-neutron measurement by Klein *et al.*[13] $C_{b\,\text{expt}}$ is to be compared with the theoretical value calculated from Eq. (3),

$$C_{b\,\text{th}} = 0.8171\ \text{rad s m}^{-1}. \tag{9}$$

Hence

$$C_{b\,\text{expt}} - C_{b\,\text{th}} = -1.59\times 10^{-2}\ \text{rad s m}^{-1}, \tag{10}$$

which is less than a 2% deviation.

It would be interesting to extend the measurement to larger values of v_b where a nonlinear term proportional to v_b^2 has to be added[11] in Eq. (3). If we assume that the experimental error can be decreased to 0.5% then the nonlinear contribution would become detectable at $v_b \simeq 10$ m s^{-1}. Specimen speeds of this order seem to be feasible in the future.

Sears[19] has pointed out that local field effects[20–22] change the λ dependence of b_c and produce a nonvanishing Fizeau effect. According to the work of Sears the effect is considerable for $\lambda > 13$ Å and small for thermal neutrons. With increased accuracy, however, the effect might become detectable for $\lambda > 4$ Å.

Financial support through the Institute Laue-

Langevin, Grenoble, and from the Bundesminister für Forschung und Technologie, Bonn, FKz 03-B56A01-9, is gratefully acknowledged.

---

[a]Also Institute Laue-Langevin, 156X Centre de Tri, 38042 Grenoble Cédex, France.

[1]H. L. Fizeau, C. R. Hebd. Seances Acad. Sci. **33**, 349 (1851).

[2]H. L. Fizeau, Ann. Chim. Phys. **57**, 385 (1859).

[3]A. Einstein, Ann. Phys. (Leipzig) **17**, 891 (1905).

[4]M. Born, *Die Relativitätstheorie Einsteins* (Springer, Berlin, 1969), 5th ed., p. 249.

[5]P. Zeeman, Proc. Acad. Sci. Amsterdam **17**, 445 (1914), and **18**, 398, 1240 (1915).

[6]P. Zeeman, Arch. Neerl. Sci. Exactes Nat., Ser 3A **10**, 131 (1927).

[7]W. M. Macek, I. R. Schneider, and R. M. Salamon, J. Appl. Phys. **35**, 2556 (1964).

[8]I. Lerche, Am. J. Phys. **45**, 1154 (1977).

[9]J.-M. Lévy-Leblond, Am. J. Phys. **44**, 271 (1976).

[10]M. A. Horne, A. Zeilinger, A. G. Klein, and G. I. Opat, Phys. Rev. A **28**, 1 (1983).

[11]U. Bonse and A. Rumpf, to be published.

[12]M. Arif, H. Kaiser, S. A. Werner, A. Cimmino, W. A. Hamilton, A. G. Klein, and G. I. Opat, Phys. Rev. A **31**, 1203 (1985).

[13]A. G. Klein, G. I. Opat, A. Zeilinger, W. Treimer, and R. Gähler, Phys. Rev. Lett. **46**, 1551 (1981).

[14]U. Bonse and M. Hart, Appl. Phys. Lett. **6**, 155 (1965).

[15]H. Rauch, W. Treimer, and U. Bonse, Phys. Lett. **A47**, 369 (1974).

[16]U. Bonse and W. Graeff, in *X-Ray Optics,* edited by H. Queisser, Topics in Applied Physics Vol. 22, (Springer-Verlag, Heidelberg, 1977), p. 93.

[17]W. Bauspiess, U. Bonse, and H. Rauch, Nucl. Instrum. Methods **157**, 495 (1978).

[18]Th. Wroblewski and U. Bonse, Nucl. Instrum. Methods Phys. Res., Sect. A **235**, 557 (1985).

[19]V. F. Sears, Phys. Rev. A **32**, 2524 (1985).

[20]M. Lax, Phys. Rev. **85**, 621 (1952).

[21]V. F. Sears, Phys. Rep. **82**, 1 (1982).

[22]M. Warner and J. E. Gubernatis, Phys. Rev. B **32**, 6347 (1985).

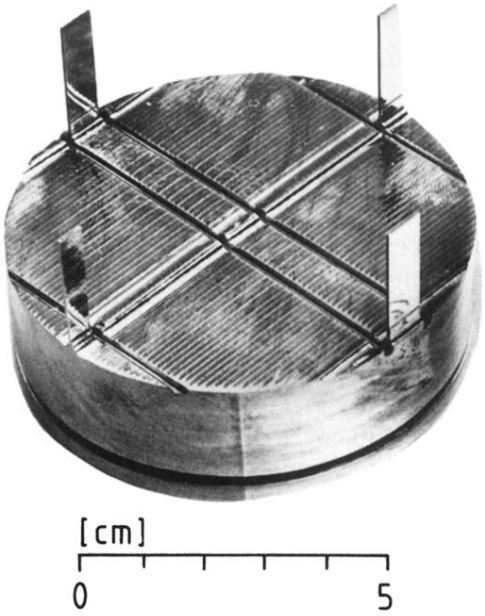

FIG. 1. Photograph of interferometer crystal.